LuxAB-based microbial cell factories for the sensing, manufacturing and transformation of industrial aldehydes

Thomas Bayer [1,2,*], Aileen Becker [1], Henrik Terholsen [1], In-Jung Kim [1], Ina Menyes [1], Saskia Buchwald [1], Kathleen Balke [1], Suvi Santala [3], Steven C. Almo [2] and Uwe T. Bornscheuer [1,*]

[1] University of Greifswald, Institute of Biochemistry, Department of Biotechnology & Enzyme Catalysis, Felix-Hausdorff-Straße 4, 17487 Greifswald, Germany
[2] Albert Einstein College of Medicine, Department of Biochemistry, 1300 Morris Park Avenue, Bronx, NY 10461-1602, USA
[3] Tampere University, Faculty of Engineering and Natural Sciences, PO Box 527 (Hervanta Campus), 33014 Tampere, Finland
* Correspondence: thomas.bayer@uni-greifswald.de (T.B.); uwe.bornscheuer@uni-greifswald.de (U.T.B)

Supplementary Information

1. General chemicals, materials and devices

Chemicals including substrates – alcohols and carboxylic acids (CAs) – and reference compounds were purchased from Sigma-Aldrich (Buchs, Switzerland), Roth (Karlsruhe, Germany) or TCI Chemicals (Tokyo, Japan) in the highest grade available, unless stated otherwise. Lysogeny broth (LB) medium and supplements including sugars (glycerol, glucose, α-lactose) and antibiotics (chloramphenicol, kanamycin, streptomycin) were ordered from Sigma-Aldrich or Roth. Salts for buffer or media solutions (e.g., KH_2PO_4, Na_2HPO_4, NaCl, $(NH_4)_2SO_4$, $MgSO_4$ or $CaCl_2$) were purchased from Sigma-Aldrich or Roth as well. Solvents were GC grade and purchased from Sigma-Aldrich or J.T. Baker (Schwerte, Germany).

Polymerase chain reactions (PCRs) were performed on a Biometra TAdvanced thermal cycler (Analytik Jena, Jena, Germany). Deoxyribonucleic acid (DNA) gels were run on a Biometra Compact XS/S system (Analytik Jena), using 1.0% (ω/v) agarose gel (Sigma-Aldrich) containing 1X SYBR® Green (Thermo Fisher Scientific, Darmstadt, Germany) in 1X TAE buffer (40 mM Trizma® base, 20 mM acetic acid, 1 mM ethylenediaminetetraacetic acid; pH ≈ 8.6). Visualization of DNA bands was done on a UV table (Shimadzu, Duisburg, Germany).

Cultivations of different *Escherichia coli* (*E. coli*) strains and whole-cell biotransformations were performed in Infors HT Multitron incubator shakers (Bottmingen, Switzerland). The optical density at 600 nm (OD_{600}) was determined with a UV-1280 spectrophotometer (Shimadzu) and cells were harvested by centrifugation using a Heraeus Fresco 17 centrifuge or a Heraeus Labofuge 400R (Thermo Fisher Scientific).

For bioluminescence measurements, a Varioskan™ LUX multimode plate reader was used (Thermo Fisher Scientific).

Gas chromatography (GC) analysis (GC-2010 Plus, Shimadzu) using a flame ionization detector (FID; Shimadzu) was performed on a ZB-5MSi column (length: 30 m; inner diameter: 0.25 mm; film thickness: 0.25 μm) from Phenomenex (Torrance, USA). GC/mass spectrometry (MS) analysis (GCMS-QP2010 SE, Shimadzu) was performed on the same column. GC methods are given below.

2. DNA manipulation and protein production methods

2.1. Sequence and ligation-independent cloning (SLIC)

The optimal annealing temperatures (T_a) were determined by gradient PCR (45–65°C), unless stated otherwise using Pfu$^+$ or *Opti*Taq DNA polymerase (Roboklon, Berlin, Germany) or Q5® high-fidelity (Q5®-HF) DNA polymerase (New England Biolabs, Frankfurt/Main, Germany). Deoxynucleotide triphosphates (dNTPs) were purchased premixed (10 mM each) from Roth. Other enzymes for the manipulation of DNA (e.g., DpnI) were purchased from Thermo Fisher Scientific or New England Biolabs. PCR products were purified with QIAquick PCR & Gel Cleanup Kit (QIAGEN, Hilden, Germany) and plasmid DNA isolated with innuPREP Plasmid Mini Kit 2.0 (Analytik Jena). DNA concentration was determined by NanoDrop™ 2000 spectrophotometer (Thermo Fisher Scientific).

Plasmids were assembled from two linear DNA fragments *via* homologous overhangs attached by PCR, following adapted protocols from Li *et al.* [1] or Wiesinger *et al.* [2]. The latter employed a seamless and ligation-independent cloning extract (SLiCE) that was prepared from *E. coli* TOP10 cultures as reported by Zhang *et al.* [3].

Sanger sequencing was performed by Eurofins Genomics (Ebersberg, Germany) with T7UP-1 F and T7term primers (**Table S9**), unless otherwise noted.

2.1.1. Cloning of the biosensor device pLuxAB

For the construction of the biosensor device, the *luxAB* coding region was amplified from pAK400c/*iluxAB_Cm*^{r}, which was previously constructed for the integration of *luxAB* into the *A. baylyi*

genome and the monitoring of intracellular levels of long-chain aldehydes (≤ C_{18}) [4, 5]. Primers introduced flanking 15 bp-overhangs complementary to the target pCDFDuet-1 vector. The pCDF backbone was amplified by primers binding upstream of the T7*lac* promoter of the multiple cloning site (MCS)-1 (R primer) and covering the unique EcoRI and SacI restriction sites (F primer), consequently, deleting the miscellaneous insert (*misc*) in the MCS-1 including its regulatory sequences but leaving the empty MCS-2 and its flanking sequences intact. Subsequently, the *luxAB* insert and the pCDF backbone were assembled by the modified SLIC procedure [2, 3], yielding pCDFduo/*luxAB*, in this study referred to as pLuxAB.

The DNA fragment encoding the *luxAB* subunits was amplified with the primer pair LuxA_T5 F/LuxB R and Pfu$^+$ (T_a = 45.0°C; **Figure S1**). The pCDF backbone was amplified with primers pCDF F/R and *Opti*Taq (T_a = 48.0°C as calculated from the primer with the lower melting temperature: $T_a = T_m - 5$ [°C]; **Figure S1**). The preparation of PCR mixtures and optimized thermal cycle conditions are given in **Table S1** and **Table S2**, respectively. The PCR products of expected sizes (pCDF ≈ 3.7 kb and *luxAB* ≈ 2.3 kb) according to agarose gel electrophoresis were purified. The correct assembly by SLiCE was confirmed by Sanger sequencing (using T5 F and DuetDOWN1 as sequencing primers; **Table S9**) of isolated plasmid DNA from single colonies of *E. coli* BL21(DE3) transformants selected on LB agar plates supplemented with 25 μg·mL^{-1} streptomycin.

Table S1. PCR mixtures for the assembly of pLuxAB

	PCR mix (Pfu$^+$)	**Final concentration**		**PCR mix** (*Opti*Taq)	**Final concentration**
5.0 μL	10X Pfu buffer	1X	5.0 μL	10X Pol B buffer	1X
2.0 μL	dNTP mix (5 mM each)	0.2 mM each	2.0 μL	dNTP mix (5 mM each)	0.2 mM each
2.5 μL	LuxA_T5 F (5 μM)	0.25 μM	2.5 μL	pCDF F (5 μM)	0.25 μM
2.5 μL	LuxB R (5 μM)	0.25 μM	2.5 μL	pCDF R (5 μM)	0.25 μM
1.0 μL	pAK400c/i*luxAB_Cm^r* (100 ng·μL^{-1})	2.0 ng·μL^{-1}	1.0 μL	pCDF/*misc* (128 ng·μL^{-1})	2.5 ng·μL^{-1}
0.9 μL	DMSO	1.8% (v/v)	0.9 μL	DMSO	1.8% (v/v)
0.5 μL	Pfu$^+$ (5 U·μL^{-1})	2.5 U	0.5 μL	*Opti*Taq (5 U·μL^{-1})	2.5 U
35.6 μL	nuclease-free water	-	35.6 μL	nuclease-free water	-

Table S2. Optimized thermal cycle conditions for the assembly of pLuxAB

PCR step (Pfu$^+$)	**Temperature** [°C]	**Time**	**No. of cycles**	**PCR step** (*Opti*Taq)	**Temperature** [°C]	**Time**	**No. of cycles**
Initial denaturation	95	5 min	1	Initial denaturation	95	5 min	1
Denaturation	95	30 s		Denaturation	95	30 s	
Annealing	45.0	30 s	30	Annealing	48.0	30 s	30
Extension	72	2 min 20 s		Extension	72	3 min 40 s	
Terminal extension	72	3 min	1	Terminal extension	72	5 min	1
Hold	10	∞	1	Hold	10	∞	1

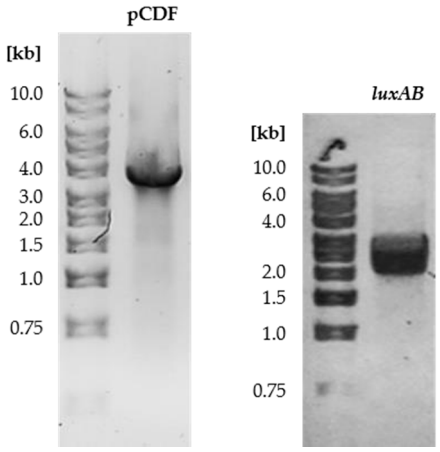

Figure S1. DNA fragments for the assembly of pLuxAB. The purified PCR products encoding the backbone (pCDF: 3.66 kb) and the insert (*luxAB*: 2.29 kb) had the expected sizes; 1 kb DNA ladder for size comparison and samples separated as described above at 120 V for 35–45 min. Irrelevant lanes were cropped, the colors of gel pictures inverted to grey scale for clarity.

2.1.2. Cloning of pACYQ/*alkJ*

The open reading frame (ORF) encoding *alkJ* was amplified from pGEc47 [6] and subcloned into a pACYC-derived backbone through SLIC as before [2, 3], replacing a miscellaneous insert (*misc*) in the target vector by the *alkJ* insert downstream of the existing T7*lac* promoter and the ribosome binding site (RBS).

The DNA fragment harboring the *alkJ* fragment was amplified with the primer pair AlkJ F/R, introducing 15 bp-overhangs complementary to the target pACYC vector, and Pfu$^+$ (T_a = 48.6°C; **Figure S2**). The pACYC backbone was amplified with the primers pACYC F/pACYC-2 R and *Opti*Taq (T_a = 48.6°C; **Figure S2**). The preparation of PCR mixtures and optimized thermal cycle conditions are given in **Table S3** and **Table S4**, respectively.

Purified DNA fragments (pACYC ≈ 4.3 kb and *alkJ* ≈ 1.7 kb) were processed and incubated with the SLiCE. Subsequently, chemically competent *E. coli* TOP10 cells were transformed with the assembly mixtures. Colonies were selected on LB agar plates containing 34 μg·mL^{-1} chloramphenicol the next day. Sanger sequencing of isolated plasmid DNA revealed a truncated ORF of the *alkJ* gene in all samples caused by the absence of a cytosine close to the C-terminus of the ORF, resulting in a frame shift and the truncation of the ADH by the last six amino acids.

Table S3. PCR mixtures for the assembly of pACYC/*alkJ*

	PCR mix (Pfu$^+$)	**Final concentration**		**PCR mix** (*Opti*Taq)	**Final concentration**
5.0 μL	10X Pfu buffer	1X	5.0 μL	10X Pol B buffer	1X
2.0 μL	dNTP mix (5 mM each)	0.2 mM each	2.0 μL	dNTP mix (5 mM each)	0.2 mM each
2.5 μL	AlkJ F (5 μM)	0.25 μM	2.5 μL	pACYC F (5 μM)	0.25 μM
2.5 μL	AlkJ R (5 μM)	0.25 μM	2.5 μL	pACYC-2 R (5 μM)	0.25 μM
1.0 μL	pGEc47 (150 ng·μL^{-1})	3.0 ng·μL^{-1}	1.0 μL	pACYC/*misc* (55 ng·μL^{-1})	1.1 ng·μL^{-1}
0.9 μL	DMSO	1.8% (v/v)	0.9 μL	DMSO	1.8% (v/v)
0.5 μL	Pfu$^+$ (5 U·μL^{-1})	2.5 U	0.5 μL	*Opti*Taq (5 U·μL^{-1})	2.5 U
35.6 μL	nuclease-free water	-	35.6 μL	nuclease-free water	-

Table S4. Optimized thermal cycle conditions for the assembly of pACYC/*alkJ*

PCR step (Pfu+)	**Temperature** [°C]	**Time**	**No. of cycles**	**PCR step** (*Opti*Taq)	**Temperature** [°C]	**Time**	**No. of cycles**
Initial denaturation	95	5 min	1	Initial denaturation	95	5 min	1
Denaturation	95	30 s		Denaturation	95	30 s	
Annealing	45.0	30 s	30	Annealing	48.0	30 s	30
Extension	72	2 min 20 s		Extension	72	3 min 40 s	
Terminal extension	72	3 min	1	Terminal extension	72	5 min	1
Hold	10	∞	1	Hold	10	∞	1

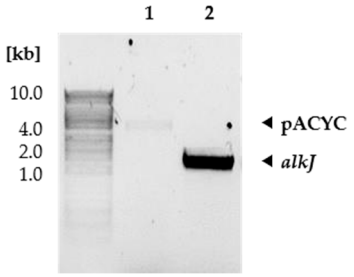

Figure S2. DNA fragments for the assembly of pACYC/*alkJ*$_{trnc}$. The purified PCR products encoding the backbone in lane 1 (pACYC: 4.30 kb) and the insert in lane 2 (*alkJ*: 1.67 kb) had the expected sizes; 1 kb DNA ladder for size comparison and samples separated on 1.2% agarose at 120 V for 20 min. Irrelevant lanes were cropped, the colors of gel picture was inverted to grey scale for clarity.

The missing cytosine was inserted by successful usage of the Q5® Site-Directed Mutagenesis Kit (New England Biolabs), yielding the desired pACYQ/*alkJ*. The insertion was performed with the primer pair AJQ5 F/R (T_a = 61.0°C as calculated by the NEBaseChanger™ tool available from: http://nebasechanger.neb.com/) and following the instructions of the supplier. The preparation of PCR mixture and the thermal cycle conditions are given in **Table S5** and **Table S6**, respectively. Finally, the completeness of the *alkJ* ORF was confirmed by Sanger sequencing (sequencing primers: **Table S9**).

Table S5. Q5® mutagenesis reaction mixture

	Q5® PCR mix	**Final concentration**
12.5 µL	Q5 Hot Start High-Fidelity 2X Master Mix	1X
2.5 µL	AJQ5 F (5 µM)	0.5 µM
2.5 µL	AJQ5 R (5 µM)	0.5 µM
1.0 µL	pACYC/*alkJ* (36 ng·µL^{-1})	1.4 ng·µL^{-1}
6.5 µL	nuclease-free water	-

Table S6. Thermal cycle conditions for Q5® mutagenesis

PCR step	Temperature [°C]	Time	No. of cycles
Initial denaturation	98	30 s	1
Denaturation	98	10 s	
Annealing	61.0	15 s	25
Extension	72	3 min 36 s	
Terminal extension	72	2 min	1
Hold	10	∞	1

2.1.3. Assembly of pACYCDuet-1/*car*$_{Mm}$:*ppt*$_{Ni}$

The pACYCDuet-1/*car*$_{Mm}$ construct harboring the *car*$_{Mm}$ gene in MCS-1 was used as template to insert the *Nocardia iowensis* phosphopantetheinyl transferase (*ppt*$_{Ni}$) gene downstream of the *car*$_{Mm}$ ORF and upstream of the MCS-2. PPTs are required to posttranslationally modify apoCAR, yielding catalytically active holoCAR [7, 8]. The *ppt*$_{Ni}$ insert was amplified from pCDF/*ppt*$_{Ni}$ including the cognate RBS. The primers introduced flanking 25 bp-overhangs for homologous recombination with the pACYCDuet-1/*car*$_{Mm}$ fragment, following the SLIC protocol by Li *et al.* [1] with a molar ratio of insert to backbone = 3:1 in the assembly mixture.

The *ppt*$_{Ni}$ insert was amplified with the primer pair Npt F/R and Q5®-HF (T_a = 57.0°C; **Figure S3**). The pACYCDuet-1 backbone harboring the *car*$_{Mm}$ gene was amplified with the primers pCAR_Npt F/R and Q5®-HF (T_a = 64.0°C; **Figure S3**). The preparation of PCR mixture and the thermal cycle conditions are given in **Table S7** and **Table S8**, respectively. The correct assembly was confirmed by Sanger sequencing of isolated plasmid DNA from single colonies of transformants selected on LB agar plates supplemented with 34 μg·mL^{-1} chloramphenicol. Sanger sequencing confirmed the correct assembly of pACYCDuet-1/*car*$_{Mm}$:*ppt*$_{Ni}$ (sequencing primers: **Table S9**).

Table S7. PCR mixtures for the assembly of pACYCDuet-1/*car*$_{Mm}$:*ppt*$_{Ni}$

PCR mix (insert)		Final concentration	PCR mix (backbone)		Final concentration
10.0 μL	5X Q5 reaction buffer	1X	10.0 μL	10X Pol B buffer	1X
2.0 μL	dNTP mix (5 mM each)	0.2 mM each	2.0 μL	dNTP mix (5 mM each)	0.2 mM each
5.0 μL	Npt F (5 μM)	0.5 μM	5.0 μL	pACYC F (5 μM)	0.25 μM
5.0 μL	Npt R (5 μM)	0.5 μM	5.0 μL	pACYC-2 R (5 μM)	0.25 μM
1.1 μL	pCDF/*ppt*$_{Ni}$ (45 ng·μL^{-1})	1.0 ng·μL^{-1}	1.1 μL	pACYC/*car*$_{Mm}$ (68 ng·μL^{-1})	1.5 ng·μL^{-1}
0.5 μL	Q5®-HF	-	0.5 μL	Q5®-HF	-
-	5X Q5 High GC enhancer	-	10.0 μL	5X Q5 High GC enhancer	1X
26.4 μL	nuclease-free water	-	16.4 μL	nuclease-free water	-

Table S8. Optimized thermal cycle conditions for the assembly of pACYCDuet-1/*car*$_{Mm}$:*ppt*$_{Ni}$

PCR step (Q5®-HF)	Temperature [°C]	Time	No. of cycles	PCR step (Q5®-HF)	Temperature [°C]	Time	No. of cycles
Initial denaturation	98	30 s	1	Initial denaturation	98	30 s	1
Denaturation	98	10 s		Denaturation	98	10 s	
Annealing	57.0	15 s	30	Annealing	64.0	15 s	30
Extension	72	18 s		Extension	72	3 min 45 s	
Terminal extension	72	2 min	1	Terminal extension	72	2 min	1
Hold	10	∞	1	Hold	10	∞	1

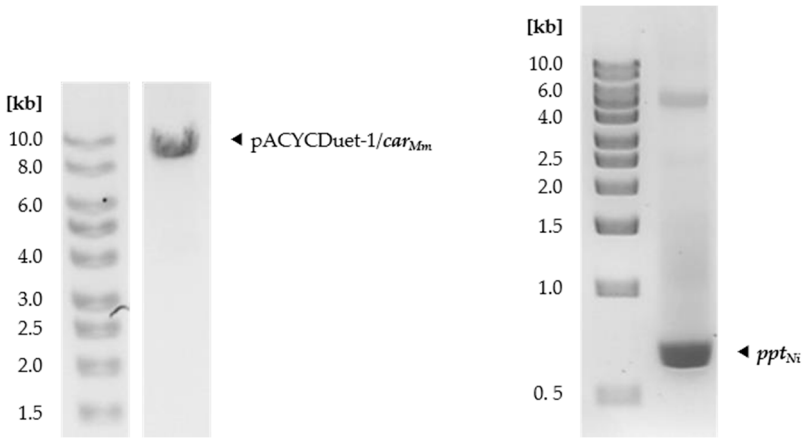

Figure S3. DNA fragments for the assembly of pACYCDuet-1/*car*$_{Mm}$:*ppt*$_{Ni}$. The purified PCR products encoding the backbone and the *car*$_{Mm}$ gene (pACYCDuet-1/car$_{Mm}$: 8.07 kb) and the insert (*ppt*$_{Ni}$: 0.63 kb) had the expected sizes. The insert was excised and purified again before assembly (not shown); 1 kb DNA ladder for size comparison and samples separated on 0.8% and 1.5% agarose, respectively, at 90–120 V for 30–45 min. Irrelevant lanes were cropped, the colors of gel pictures inverted to grey scale for clarity.

2.2. Cloning of pET28a/*co-6*$_{Ac}$

The gene encoding the choline oxidase variant 6 from *Arthrobacter chlorophenolicus* (CO-6$_{Ac}$; B8H740) was based on the work by Heath *et al.* [9]. For the expression in *E. coli*, it was codon-optimized and synthesized by BioCat GmbH (Heidelberg, Germany). The gene was sub-cloned by SLIC into the vector pET28a in optimal distance to the RBS by the BioCat GmbH as well.

2.3. List of primers

Desalted DNA oligonucleotides were ordered from Invitrogen/Thermo Fisher Scientific and dissolved in nuclease-free water (Invitrogen, Darmstadt, Germany). The resulting stock solutions (100 µM) were further diluted and used as primers for polymerase chain reactions (PCRs; 5 µM) or Sanger sequencing (10 µM).

Table S9. List of DNA oligonucleotides used in this study

Primer	Sequence (5′ → 3′)	Purpose
LuxA_T5 F LuxB R pCDF F pCDF R	CCTGCATTAGGAAATAGTATATGCTGAACTTTCTTC GAATTCTTAGGTATATTCCATGTGGTACTTCT TATACCTAAGAATTCGAGCTC ATTTCCTAATGCAGGAGTC	Assembly (2 fragments): pCDFduo/*luxAB* (pLuxAB)
AlkJ F AlkJ R pACYC F pACYC-2 R	GAAGGAGATATACATATGTACGACTATATAATCGTTGG GTTAGCAGCCGGATCCTTACATGCAGACAGCTATCATG GATTATATAGTCGTACATATGTATATCTCCTTCTTAAAGTTAAAC GATAGCTGTCTGCATGTAAGGATCCGGCTGCTAAC	Assembly (2 fragments): pACYC/*alkJ*
AJQ5 F AJQ5 R	CCATGATAGCTGTCTGCATG CCAACTCTAGCTCTGCAC	Restoring *alkJ* ORF, yielding pACYQ/*alkJ*
mAlkJ F	CACCTTCTAATGCTTTCTG	SEQ (F); binds within the *alkJ* ORF
Npt F Npt R pCAR_Npt F pCAR_Npt R	ATGATTGAAACCATCCTGCCGGC TCACGCGTAAGCAATAGCGGTC TGACCGCTATTGCTTACGCGTAACTTAAGTCGAACAGAAAGTAATCG CCGGCAGGATGGTTTCAATCATGGTATATCTCCTTTTATTAGCGGC	Assembly (2 fragments): pACYCDuet-1/car_{Mm}:ppt_{Ni}
mCAR1	GTTACTTCCTGACCGAT	SEQ (F); binds within the car_{Mm} ORF
mCAR2	CATGCACACTCGCAAACG	SEQ (R); binds within the car_{Mm} ORF
mCAR3	GCATGATCCTTAGCTTAG	SEQ (F); binds within the car_{Mm} ORF
T7UP-1	CCAGCAACCGCACCTGTG	SEQ (F); binds upstream of the T7*lac* promoter
T7term	GCTAGTTATTGCTCAGCGG	SEQ (R); binds upstream of the T7 terminator
T5 F	GTGAGCGGATAACAATTTG	SEQ (F); binds to the T5 promoter region
ACYCDuetUP1	GGATCTCGACGCTCTCCCT	SEQ (F); standard primer for MSC-1 inserts in Duet vectors
DuetDOWN1	GATTATGCGGCCGTGTACAA	SEQ (R); standard primer for MSC-1 inserts in Duet vectors

SEQ = primer for Sanger sequencing, forward (F) or reverse (R); ORF = open reading frame; MSC = multiple cloning site

2.4. List of strains and plasmids

Table S10. List of strains and plasmids used in this study

E. coli strain	*Genotype*	Reference
BL21(DE3)	*F⁻ ompT gal dcm hsdSB* (r_B^-, m_B^-) *(DE3)*	Thermo Fisher Scientific
DH5α	*F⁻ endA1 recA1 endA1* Φ80*lacZ*ΔM15 Δ(*lacZYA-argF*) U169 *hsdR17*(r_K^-, m_K^+) *phoA supE44 thi-1 gyrA96 relA1* λ⁻	Thermo Fisher Scientific
TOP10	*F⁻ mcrA Δ(mrr-hsdRMS-mcrBC)* Φ80*lacZΔM15 Δ(lac)X74 recA1 araD139 Δ(ara-leu)7697 galU galK rpsL* (Str^R) *endA1 nupG*	Thermo Fisher Scientific
RARE	*E. coli* K-12 MG1655 Δ*(dkgA, dkgB, yeaE, yjgB, yqhC, yqhD, yahK)*	[10]

Table S10. List of strains and plasmids used in this study (continued)

Plasmid	*Genotype; antibiotic markers* [a]	Reference (accession no.)
pACYCDuet-1/*car*$_{Mm}$	*car*$_{Mm}$; *Cm*^{R}	This study (*car*$_{Mm}$: WP_012393886)
pACYCDuet-1/*car*$_{Mm}$:*ppt*$_{Ni}$	*car*$_{Mm}$ *ppt*$_{Ni}$; *Cm*^{R}	This study (*car*$_{Mm}$: WP_012393886) (*ppt*$_{Ni}$: ABI83656)
pACYC/*alkJ*$_{trnc}$ [b]	*alkJ*$_{trnc}$; *Cm*^{R}	This study
pACYQ/*alkJ*	*alkJ*; *Cm*^{R}	This study (*alkJ*: Q00593)
pAK400c/*iluxAB*	*luxAB*; *Cm*^{R}	[4]
pCDF/*ppt*$_{Ni}$	*ppt*$_{Ni}$; *Str*^{R}	This study (*ppt*$_{Ni}$: ABI83656)
pCDFduo/*luxAB* (pLuxAB)	*luxAB*; *Str*^{R}	This study (*luxA*: WP_088373098) (l*uxB*: P19840)
pET28a/*co-6*$_{Ac}$	*co-6*$_{Ac}$; *Kan*^{R}	[9] (*co*$_{Ac}$: B8H740) [c]
pGEc47	*alkBFGHJKL alkST*; *Tet*^{R}	[6]

[a] Antibiotic markers: *Cm*^{R} (chloramphenicol), *Str*^{R} (streptomycin), *Kan*^{R} (kanamycin), *Tet*^{R} (tetracycline); see also: [11]

[b] The ORF of the *alkJ* gene was truncated by the last six amino acids of the C-terminus (*alkJ*$_{trnc}$). This was caused by the absence of a cytosine, which resulted in a frame shift as determined by Sanger sequencing. The cytosine was inserted by Q5® site-directed mutagenesis and the complete ORF restored, yielding pACYQ/*alkJ*.

[c] The accession number refers to the wildtype enzyme.

2.5. Preparation of chemically competent *E. coli* cells and transformation by heat-shock

Chemically competent *E. coli* cells were produced by well-established protocols using $CaCl_2$ (0.1 M) and transformed with plasmid DNA (25–100 ng·µL^{-1}) by heat-shock at 42°C for 45 s (e.g., [2] and references therein). For the efficient transformation of *E. coli* RARE cells, plasmids were passed through *E. coli* DH5α. Briefly, a single colony of the strain to be transformed was grown in liquid LB (25 g·L^{-1}) containing the appropriate antibiotic if applicable at 37°C with shaking (180 rpm) for 12–16 h. Fresh LB medium supplemented with antibiotic if applicable was inoculated with 1.0% (v/v) preculture in a baffled flask and incubated at 37°C with shaking (180 rpm) until an OD_{600} = 0.2–0.4 was reached. The culture was dispensed into 1.5 mL aliquots and centrifuged (6 000 x g, 4°C) for 15 min. The following steps were performed on ice. The supernatant was removed. The cell pellet was resuspended in ice-cold 0.1 M $CaCl_2$ (0.5 mL) and incubated for 15 min. It was centrifuged (3 000 x g, 4°C) for 10 min. The supernatant was removed and the cell pellet resuspended in 0.1 mL ice-cold $CaCl_2$ solution. Plasmid DNA (1 µL) was added and the resulting mixture incubated on ice ≥ 1 h before the heat-shock was performed. The transformation mixture was put back on ice for 2 min. For recovery, 0.5 mL SOC medium (2% tryptone, 0.5% yeast extract, 10 mM NaCl, 2.5 mM KCl, 10 mM $MgCl_2$, 10 mM $MgSO_4$ and 20 mM glucose) were added. It was incubated at 37°C with vigorous shaking for ≥ 1 h. Selection of transformants was performed in LB medium (or on LB agar plates containing 1.5% agar-agar) in the presence of the appropriate antibiotic(s).

The following final concentrations of antibiotics were used in this study: chloramphenicol (34 µg·mL^{-1}), kanamycin (50 µg·mL^{-1}) and streptomycin (25 µg·mL^{-1}). Only half the concentration was used for the selection and subsequent cultivation of strains harboring two plasmids.

2.6. Protein production/analysis and preparation of resting cells (RCs)

Protein production (AlkJ, CAR$_{Mm}$/PPT$_{Ni}$, CO-6$_{Ac}$ and LuxAB) was performed in *E. coli* RARE transformants cultivated in auto-induction medium (AIM; 2.5% LB medium, 1 mM $MgSO_4$, 25 mM $(NH_4)_2SO_4$, 50 mM KH_2PO_4, 50 mM Na_2HPO_4, 5% glycerol, 0.5% glucose, 2% α-lactose) adapted from

Studier [12]. Therefore, a single colony of the desired strain (or transformant) was grown in LB medium (25 g·L^{-1}) containing the appropriate antibiotic(s) at 37°C with shaking (180 rpm) for 12–16 h. AIM supplemented with antibiotic(s) was inoculated with 0.2% (v/v) preculture in baffled flasks and incubated at 37°C with shaking (180 rpm) for 4–6 h (6 h for co-transformants, 5 h for pLuxAB transformants and 4 h for all others). Enzyme production was performed at 20°C with shaking (150 rpm) for 16–20 h.

Cells were harvested by centrifugation (6 000 x g, 4°C) for 20 min. The cell pellet was resuspended in resting cell medium (RCM; 22 mM KH_2PO_4, 42 mM Na_2HPO_4, 8.56 mM NaCl, 1 mM $MgSO_4$, 1 mM $CaCl_2$, 1% glucose) until an OD_{600} = 10.0 was reached. RCs were used on the day of preparation for the LuxAB-based aldehyde assay and biotransformations as described below.

Protein expression was confirmed by 12.5% (ω/v) sodium dodecyl sulfate-polyacrylamide gel electrophoresis (SDS-PAGE) analysis under reducing conditions of whole-cell samples normalized to OD_{600} = 7.0; standard protocols were followed (e.g., [2]) using the Mini-PROTEAN electrophoresis system (Bio-Rad, Feldkirchen, Germany). To visualize protein bands, gels were stained with InstantBlue™ Protein Stain (Expedeon, Heidelberg, Germany) at room temperature for ≥ 15 min. Exemplary SDS-PAGE gels are shown in **Figure S4**.

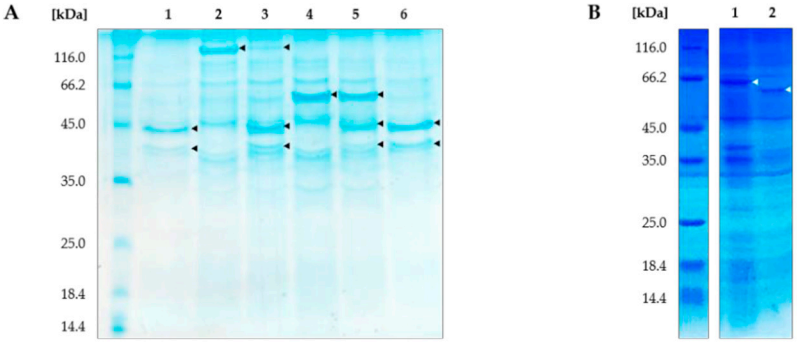

Figure S4. SDS-PAGE analysis of whole-cell samples. (**A**) Expression of (**1**) LuxAB [LuxA: 41 kDa, LuxB: 37 kDa], (**2**) CAR_{Mm} [129 kDa] and PPT_{Ni} [23 kDa; poor expression], (**3**) CAR_{Mm}/PPT_{Ni} and LuxAB, (**4**) AlkJ [62 kDa], (**5**) AlkJ and LuxAB, and (**6**) $CO\text{-}6_{Ac}$ [63 kDa; poor expression] and LuxAB in *E. coli* RARE. (**B**) Expression of (**1**) $CO\text{-}6_{Ac}$ [63 kDa] and (**2**) AlkJ [62 kDa] in *E. coli* RARE. Sample loading normalized to OD_{600} = 7.0 and SDS-PAGE analysis performed as described above. Staining performed for (**A**) 30 min and (**B**) 16 h; gels were rinsed with deionized water before documentation. Irrelevant lanes were cropped, the contrast of both pictures was increased by 20%; (◄) indicate protein bands of interest.

3. LuxAB-based high-throughput (HT) assay for aldehyde detection (96-well plate format)

3.1. Direct detection of aldehydes by LuxAB

RCs expressing LuxAB were prepared as described above. In 96-well plates (flat bottom, black polystyrene; Greiner Bio-One, Frickenhausen, Germany), the following mixtures were prepared: (i) 2 µL stock solution of the desired aldehyde (100 mM in dimethyl sulfoxide or ethanol) or (ii) 2 µL 1:10-diluted stock solution (10 mM in ethanol) were added to 198 µL RCs (OD_{600} = 10.0) per well (V_{total} = 200 µL containing 1% (v/v) organic co-solvent). It was mixed gently and the bioluminescence measured immediately. The change in bioluminescence was followed at 25°C up to 1 h and after 24 h.

The following aldehydes were tested: octanal (**2b**), nonanal (**3b**), decanal (**4b**), citral (**15b**; applied as a commercial mixture of the *E*- and *Z*-isomers geranial and neral), the (*R*)- and (*S*)-enantiomers of citronellal (**16b**), melonal (**17b**), benzaldehyde (**18b**), 2-phenyl ethanal (**19b**), cuminaldehyde (**20b**), *trans*-cinnamaldehyde (**21b**), 3-phenyl propanal (**22b**), 2-methylbenzaldehyde (**23b**), 3-methylbenzaldehyde (**24b**) and 4-methylbenzaldehyde (**25b**). The increase in bioluminescence in the presence of (i) 1 mM aldehyde is discussed in the main article (**Figure 2**), the results for (ii) 0.1 mM aldehyde are shown in **Figure S5**.

To assess the fold increase in bioluminescence above background (b_x) emitted by LuxAB in the presence of aldehyde substrates, the following equation was used:

$$b_x = \frac{t_x}{t_0},$$

where t_x is the blank-corrected bioluminescence signal at the corresponding time point x and t_0 is the blank-corrected bioluminescence signal before the addition of substrate; t_0 is determined by the addition of 1% (v/v) organic co-solvent and measuring the bioluminescence immediately. The blank value is defined as the bioluminescence detected in RCs before the addition of any organics.

Supplementation of the aldehydes **2–4b** increased the bioluminescence roughly 8 300-, 10 200- and 27 000-fold, respectively, after 3 min (**Figure S5A**). Even at the lower concentration of 0.1 mM aldehyde, this set-up was sufficient to confirm the initially reported substrate scope of LuxAB in *P. luminescens* [13].

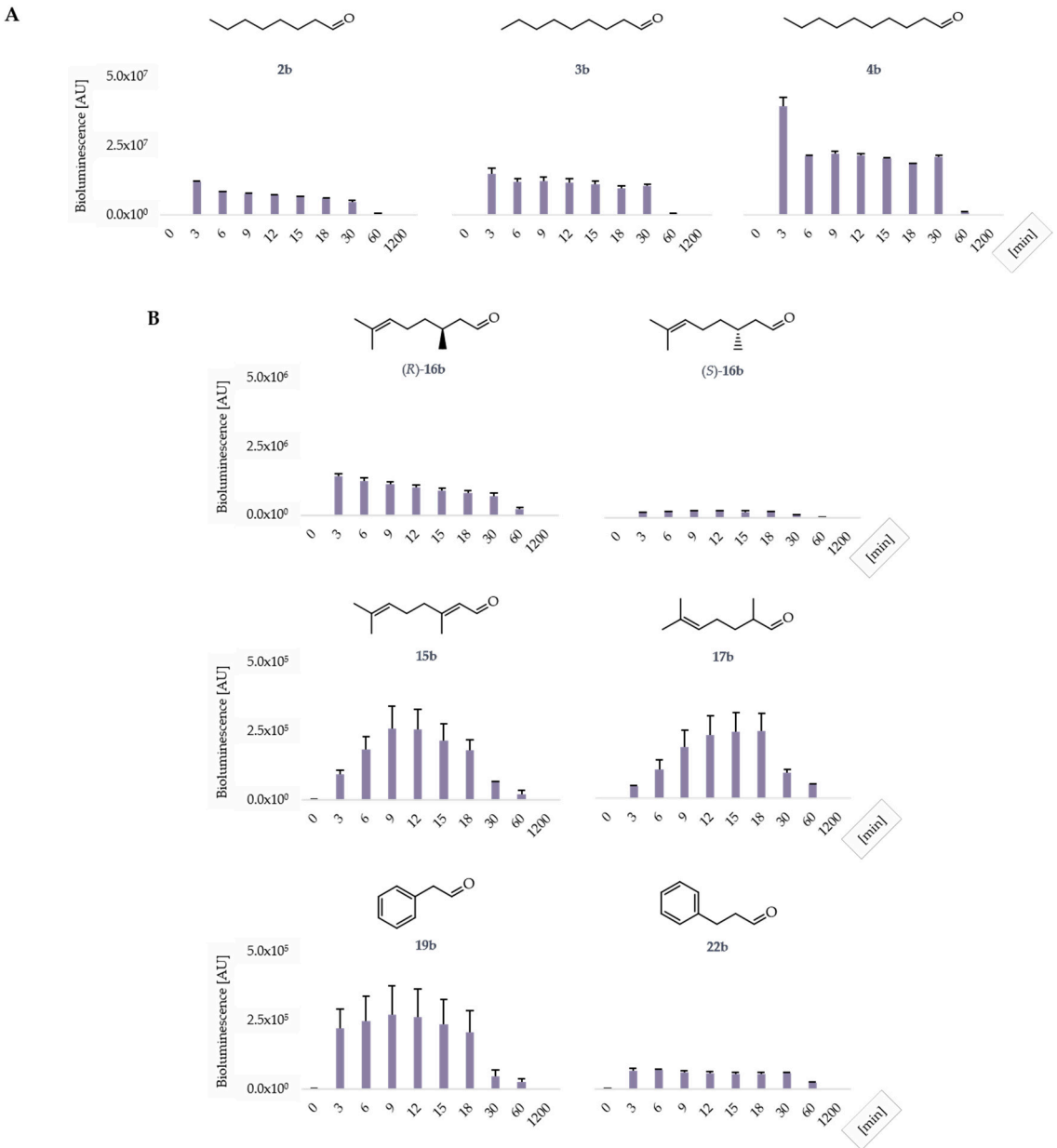

Figure S5. LuxAB-based detection of aldehydes at low concentration in *E. coli*. (**A**) The bioluminescence greatly increased in the presence of previously reported aliphatic aldehydes (**2–4b**). (**B**) New substrates of LuxAB included monoterpene aldehydes (**15–17b**) and aromatic aldehydes with aliphatic sidechains (**19b** and **22b**). Differences in maximal bioluminescence indicate aldehyde preference of LuxAB. Experiments performed in RCs of *E. coli* RARE (OD_{600} = 10.0) expressing LuxAB from pLuxAB in the presence of 0.1 mM aldehyde and 1% (v/v) ethanol as co-solvent; data presented as mean values + standard deviation (SD) of biological replicates (n = 3).

The tested terpene aldehydes increased the bioluminescence; the clear preference of LuxAB for the (*R*)-enantiomer of **16b** could be confirmed (**Figure S5B**; see also: **Figure 2B** in the main article). (*R*)-**16b** and **17b**, for example, increased the bioluminescence almost 1 000- and 270-fold, respectively, after 9 min. The aromatic aldehydes **19b** and **22b** also yielded bioluminescence (188- and 48-fold increase after 9 min and 6 min, respectively; **Figure S5B**), whereas **18b**, **20–21b** (data not shown) and the tolualdehydes **23–25b** (**Figure S6**) did not under these conditions.

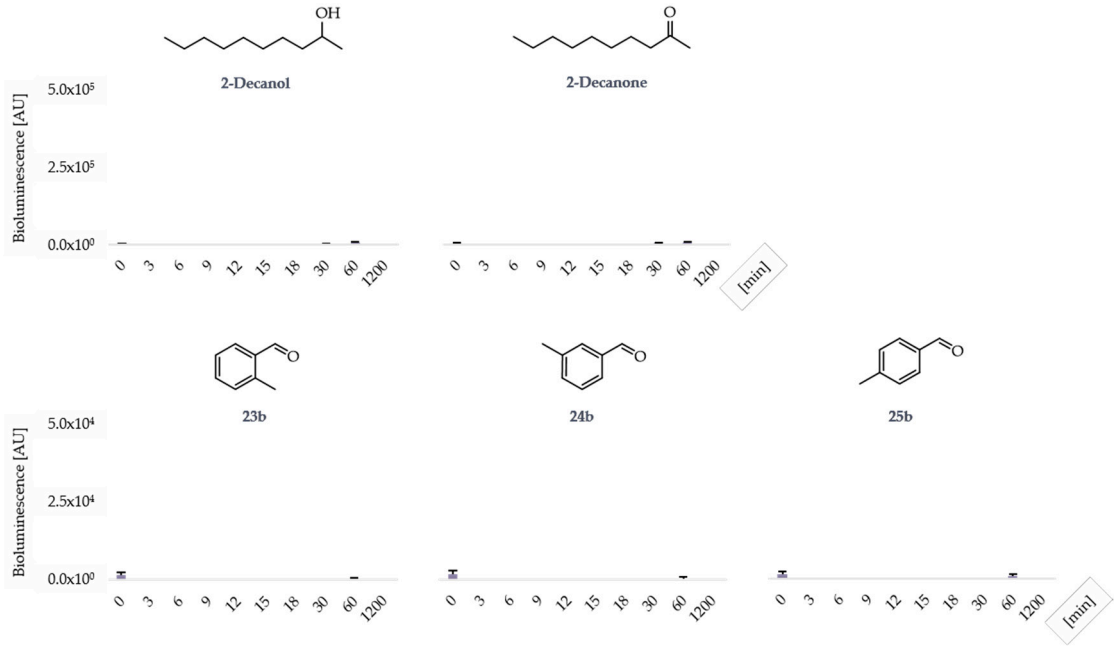

Figure S6. LuxAB-based detection of aldehydes in *E. coli* (background and negative controls). In the presence of 2-decanol and 2-decanone (negative controls), the bioluminescence did not increase significantly (top). The direct addition of certain aromatic aldehydes did not increase the bioluminescence either, exemplarily shown for **23–25b** (bottom). Experiments performed in RCs of *E. coli* RARE (OD_{600} = 10.0) expressing LuxAB from pLuxAB in the presence of 0.1 mM organic compound if applicable and 1% (v/v) ethanol as co-solvent; data presented as mean values + standard deviation (SD) of biological replicates (n = 3).

3.2. Enzymatic production of aldehydes by oxidoreductases and detection by LuxAB

RCs co-expressing LuxAB and the oxidoreductase of interest (AlkJ, CAR_{Mm} or $CO\text{-}6_{Ac}$) were prepared as described above. In 96-well plates (flat bottom, black polystyrene; Greiner Bio-One), 2 µL stock solution of the desired substrate (100 mM in dimethyl sulfoxide or ethanol) were added to 198 µL RCs (OD_{600} = 10.0) per well (V_{total} = 200 µL; containing 1 mM substrate and 1% (v/v) organic co-solvent). It was mixed gently and the bioluminescence measured immediately. The change in bioluminescence was followed at 25°C up to 1 h (**Figure 3** in the main article).

To assess the fold increase in bioluminescence (b_x) above background caused by the enzymatic production of aldehydes from oxidoreductase substrates, the blank-subtracted bioluminescence signal at the corresponding time point (t_x) was divided by the bioluminescence signal before the addition of substrate (t_0) as before. Since the bioluminescence slightly increased over time in the sole presence of 1% (v/v) organic co-solvent, it was monitored in parallel and the fold increase calculated as before. This yielded the cut-off value at t_x. Substrate-enzyme combinations exhibiting bioluminescence greater than the cut-off value + SD, referred to as the experimental cut-off (XCO) in this study (**Figure S7**), were re-screened in whole-cell biotransformations expressing the corresponding oxidoreductase alone as described below.

Since XCO can vary (e.g., expression levels of target enzymes, temperature, cell viability) its determination was crucial to distinguish increasing b_x from the *in situ* production of aldehydes and from the unspecific increase in the presence of organic co-solvents like ethanol (**Figure S7B–D**).

A

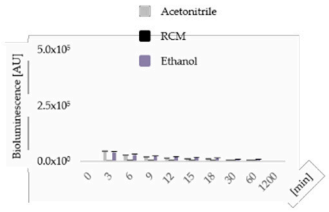

[min]	b_{ACN}	b_{RCM}	b_{EtOH}
0	1.0	1.0	1.0
3	2.0	0.2	1.8
6	1.2	0.2	1.3
9	0.8	0.2	1.0
12	0.6	0.2	0.8
15	0.5	0.2	0.7
18	0.4	0.2	0.6
30	0.3	0.2	0.4
60	0.2	0.2	0.4
1200	0.0	0.2	0.0

B

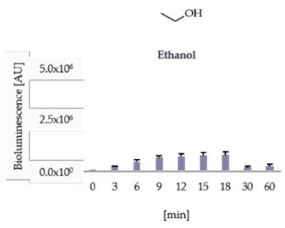

[min]	b_{EtOH}	SD	XCO-1	b_{EtOH}	SD	XCO-2
0	1.0	0.2	1.2	1.0	0.2	1.2
3	9.5	1.3	10.8	4.6	2.4	6.9
6	20.9	3.2	24.0	2.5	1.4	3.9
9	28.3	4.3	32.7	2.1	1.1	3.3
12	32.0	5.9	37.9	1.9	0.9	2.8
15	33.7	5.8	39.5	1.9	0.7	2.6
18	35.0	6.2	41.1	1.8	0.6	2.4
30	8.2	3.2	11.4	0.8	0.1	0.9
80	10.2	4.7	14.9	1.4	0.1	1.5

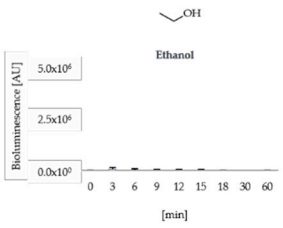

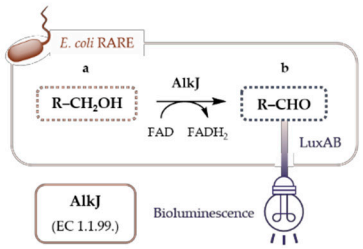

[min]	XCO-1	**4a**	(*R*)-**16a**	XCO-2	**21a**	**24a**
0	1.2	< XCO	< XCO	1.2	< XCO	< XCO
3	10.8	8266.7	< XCO	6.9	< XCO	< XCO
6	24.0	8101.9	< XCO	3.9	< XCO	< XCO
9	32.7	7754.1	< XCO	3.3	15.0	< XCO
12	37.9	7765.3	< XCO	2.8	43.8	< XCO
15	39.5	7743.0	< XCO	2.6	81.3	< XCO
18	41.1	7712.7	< XCO	2.4	110.1	< XCO
30	11.4	8973.2	25.6	0.9	119.3	6.2
80	14.9	9280.7	232.2	1.5	50.1	14.2

C

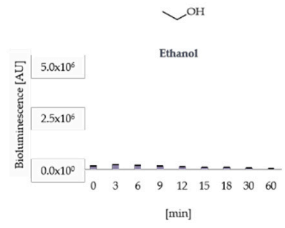

[min]	b_{EtOH}	SD	XCO
0	1.0	0.0	1.0
3	1.3	0.1	1.4
6	1.1	0.1	1.2
9	0.9	0.1	1.0
12	0.8	0.1	0.9
15	0.7	0.1	0.8
18	0.7	0.0	0.7
30	0.5	0.0	0.5
80	0.4	0.1	0.5

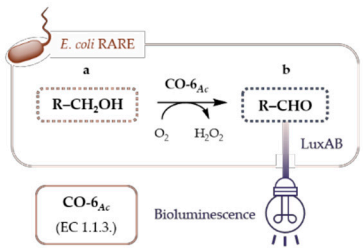

[min]	XCO	**3a**	(*R*)-**16a**	**21a**	**24a**
0	1.0	< XCO	< XCO	< XCO	< XCO
3	1.4	15.4	23-1	< XCO	< XCO
6	1.2	35.6	37.7	< XCO	< XCO
9	1.0	39.7	41.6	< XCO	< XCO
12	0.9	41.3	43.1	2.0	< XCO
15	0.8	42.5	45.0	2.0	< XCO
18	0.7	44.8	45.3	5.7	< XCO
30	0.5	74.9	22.9	2.1	< XCO
80	0.5	97.0	10.1	5.7	< XCO

Figure S7. Background luminescence and determination of the XCO value. (**A**) The bioluminescence above background transiently increased in the presence of 1% (v/v) organic co-solvents like ethanol (b_{EtOH}) and acetonitrile (b_{ACN}) after 3–6 min – but not in RCM (b_{RCM}) – in RCs expressing LuxAB from pLuxAB. Contrary, the bioluminescence increased in the presence of organic co-solvents, exemplarily shown for ethanol (b_{EtOH}; **B–D**), in RCs co-expressing LuxAB and one of the oxidoreductases. Both XCO values and b_x, shown for the selected oxidoreductase substrates **3**, *(R)*-**16**, **21** and **24**, were calculated as described in this study from biological replicates (n = 3) and used for the assessment of the HT assay (**Figure 3** in the main article). (**B**) Change in bioluminescence in RCs co-expressing LuxAB and AlkJ (pACYQ/*alkJ*), producing aldehydes (**b**) from primary alcohols (**a**); XCO-1 (left) and XCO-2 (right) for two separately performed HT assays. (**C**) Change in bioluminescence in RCs co-expressing LuxAB and CO-6_{Ac} (pET28a/*co-6*$_{Ac}$), producing aldehydes (**b**) from primary alcohols (**a**). (**D**) Change in bioluminescence in RCs co-expressing LuxAB and CAR_{Mm} (pACYCDuet-1/*car*$_{Mm}$:*ppt*$_{Ni}$), producing aldehydes (**b**) from CAs **c**); PPT_{Ni} for posttranslational modification of CAR_{Mm} omitted for clarity. The Enzyme Commission (EC) numbers were adapted from: https://www.brenda-enzymes.org/. All data produced in RCs *E. coli* RARE (OD_{600} = 10.0) in the presence of 1% (*v*/*v*) co-solvent and 1 mM substrate if applicable; b_x presented as mean fold increase in bioluminescence based on biological replicates (n = 3).

D

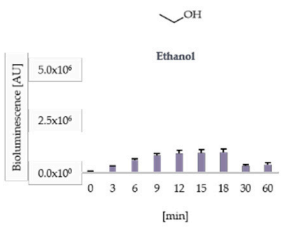

[min]	b_{EtOH}	SD	XCO
0	1.0	0.0	1.0
3	1.3	0.1	1.4
6	1.1	0.1	1.2
9	0.9	0.1	1.0
12	0.8	0.1	0.9
15	0.7	0.1	0.8
18	0.7	0.0	0.7
30	0.5	0.0	0.5
80	0.4	0.1	0.5

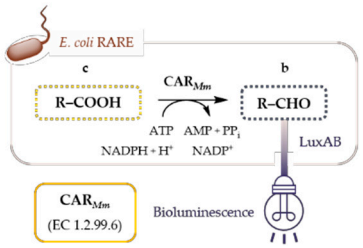

[min]	XCO	**4c**	(*R*)-**16c**	**21c**	**24c**
0	1.0	< XCO	< XCO	< XCO	< XCO
3	4.9	704.4	16.3	< XCO	< XCO
6	10.5	817.0	70.4	22.2	< XCO
9	14.6	868.6	88.9	25.9	< XCO
12	16.9	878.4	85.1	21.9	< XCO
15	17.6	879.5	75.9	16.4	< XCO
18	18.1	871.7	64.3	11.3	< XCO
30	6.0	913.2	55.9	< XCO	< XCO
80	7.8	989.3	67.5	< XCO	< XCO

Figure S7. Background luminescence and determination of the XCO value (continued). Change in bioluminescence over time in response to the *in situ* production of aldehydes (**b**) by CAR$_{Mm}$ from **4c**, *(R)*-**16c**, **21c** and **24c**; PPT$_{Ni}$ omitted for clarity. The XCO was calculated as described in this study and was used to assess the increase in bioluminescence caused by the presence of aldehydes and not the unspecific increase in the presence of organic co-solvents such as ethanol.

4. Biotransformations and GC analysis

4.1. Whole-cell biotransformations, sampling and GC analysis

RCs (OD_{600} = 10.0) expressing the oxidoreductase of interest or co-expressing LuxAB and AlkJ for cascade reactions were prepared as described above. Whole-cell biotransformations were performed in glass vials with screw-caps (4 mL) at 5 mM substrate concentration for alcohols and carboxylates in the presence of 5% (v/v) organic co-solvent (V_{total} = 0.5 mL) at 25°C (220–250 rpm) for 0–24 h. For GC analysis, samples (100 µL) of the biotransformation mixtures were taken immediately after the addition of substrate and mixing (t ≈ 0 h), 1 h and 24 h. Unless for biotransformations involving monoterpenoid aldehydes (e.g., **15b**) and related compounds [14], samples were acidified with 2 M HCl (10 µL) and extracted two times with ethyl acetate (200 µL) containing 1 mM methyl benzoate as internal standard (IS). Extraction was performed by vortexing for 30–45 s. It was centrifuged (13 000 x g, 4°C) for 1 min after extraction to separate the aqueous and the organic phase. The combined organic phases were dried over Na_2SO_4 and transferred into a GC vial with insert, capped and submitted to GC analysis. Compound identification was performed by the comparisons of retention times of commercial standards (**Table S11**), unless stated otherwise. For GC analysis, the following methods were used: GC/FID (hydrogen, 0.96 mL·min^{-1} flow rate; injector and detector: 300°C; 100°C, hold 1 min, 20°C per min to 250°C, hold 5 min; total time: 13.5 min) or GC/MS (helium, 1.00 mL·min^{-1} flow rate; injector: 280°C, ion source and interface: 260°C; 100°C, hold 5 min, 20°C per min to 250°C, hold 5 min, 20°C per min to 280°C, hold 5 min; total time: 24.0 min).

GC yields were calculated by standard calibrations using linear regression (**Table S11**) or employing relative response factors (RRFs; **Table S11**). The RRFs were calculated as follows:

$$RFF_X = \frac{RF_X}{RF_{IS}} = \frac{\frac{Peak\ area\ X}{c_X}}{\frac{Peak\ area\ IS}{c_{IS}}},$$

whereas RF_X is the response factor of compound X and RF_{IS} is the response factor for the IS. Compound solutions and the IS were measured at 1 mM final concentration and the resulting peak areas were used to calculate the RRFs. Finally, the mean RRFs (n ≥ 2) were applied to calculate GC yields.

4.1.1. Reduction of aromatic carboxylic acids by CAR*Mm*/PPT*Ni*

RCs of *E. coli* RARE (OD600 = 10.0) co-expressing CAR*Mm*/PPT*Ni* were produced as described above. The *ortho-*, *meta-* and *para*-substituted **23–25c** were reduced to 2-methylbenzaldehyde (**23b**), 3-methylbenzaldehyde (**24b**) and **25b**, respectively. Long reaction times also lead to the re-oxidation of the aldehydes to the corresponding CA (**Figure S8**).

The aldehydes **23b** and **24b** are poor substrates for LuxAB, hence, could not be unambiguously detected in the HT assay (**Figure 3D** in the main article). Consequently, the aldehyde detection scope of LuxAB represents a limitation of the HT assay.

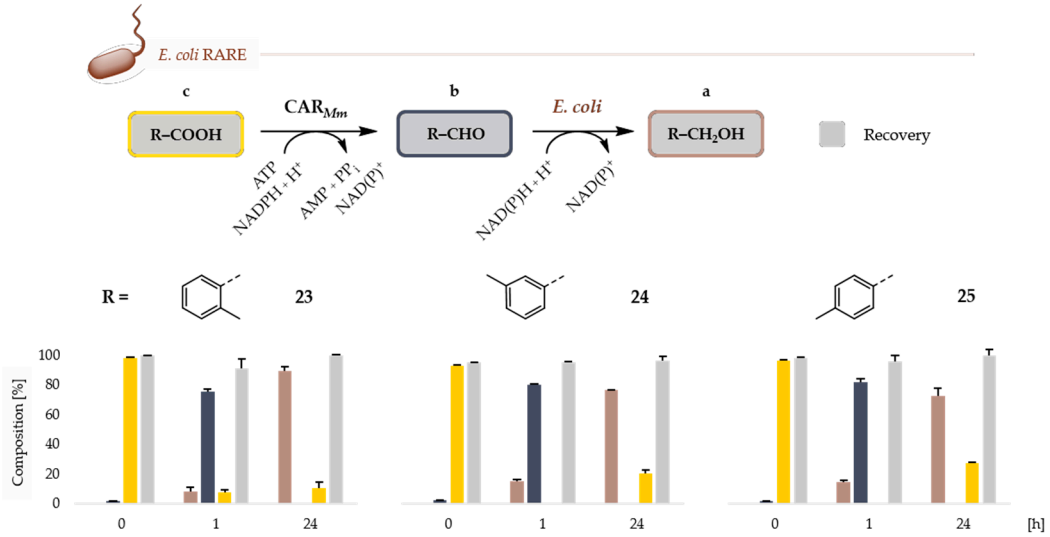

Figure S8. Enzymatic reduction of toluic acids by CAR*Mm*. Reduction of **23–25c** to the target aldehydes (**b**) and further reduction to the corresponding alcohols (**a**) by endogenous ADHs. PPT*Ni* for the posttranslational modification of CAR*Mm* was omitted for clarity. Experiments were performed in RCs of *E. coli* RARE (OD600 = 10.0) expressing CAR*Mm*/PPT*Ni* from pACYCDuet-1 in the presence of 5 mM CA (**c**) and 5% (v/v) organic co-solvent. Sampling: 0 h (after the addition of substrate and mixing), 1 h and 24 h. Reduced recoveries attributed to low solubility in RCM, volatility and/or metabolization of compounds; 100% recovery represents the complete retrieval of the amount of substance added. GC yields presented as mean values + SD [%] of biological replicates (n ≥2).

4.1.2. Production of (monoterpene) aldehydes by CAR*Mm*/PPT*Ni* and transformation *in vivo*

RCs of *E. coli* RARE (OD600 = 10.0) co-expressing CAR*Mm*/PPT*Ni* were produced as before. The CAs **15c**, (*R*)- and (*S*)-**16c** were successfully reduced to the corresponding aldehydes (**b**; **Table S12**). Observed byproducts (indicated in red) included the corresponding alcohols (**a**), formed by the further reduction of aldehydes by endogenous ADHs. Other byproducts such as **15c** – formed from **16c** – indicate enoate reductase and aldehyde dehydrogenase host activities. The fatty acid **4c** was also reduced to **4b** by CAR*Mm* and further to **4a** by endogenous enzymes; metabolites from fatty acid synthesis or degradation were not detected under these conditions (**Figure 5** in the main article).

Table S11. Production of (monoterpene) aldehydes by CAR*Mm* and transformation *in vivo*

	Time	15c	15b	15a	16c	16b	Recovery [a]
Reduction of **15c**	0	52.2 ± 2.9 [b]	n.d.	n.d.	7.3 ± 2.0	n.d.	59.8 ± 1.4
	1	45.1 ± 1.3 [b]	37.5 ± 0.6	10.5 ± 0.2	6.2 ± 1.8	1.5 ± 1.0	98.6 ± 0.9
	24	n.d.	49.0 ± 2.7	22.9 ± 1.1	n.d.	11.0 ± 0.8	82.9 ± 4.6

	Time	16c	16b	16a	15c		Recovery [a]
Reduction of (*R*)-**16c**	0	75.8 ± 2.4	n.d.	n.d.	n.d.	-	75.8 ± 2.4
	1	44.1 ± 1.0	53.1 ± 2.5	n.d.	n.d.		97.2 ± 1.5
	24	n.d.	76.1 ± 2.2	9.9 ± 1.3	8.6 ± 0.5		94.6 ± 2.6

Table S11. Production of (monoterpene) aldehydes by CAR*Mm* and transformation *in vivo* (continued)

	Time	16c	16b	16a	15c		Recovery [a]
Reduction of (*S*)-**16c**	0	48.8 ± 3.9	n.d.	n.d.	n.d.	-	48.8 ± 3.9
	1	46.5 ± 11.8	52.9 ± 12.5	n.d.	n.d.		99.3 ± 1.1
	24	n.d.	63.9 ± 10.3	4.9 ± 3.5	10.1 ± 1.2		78.8 ± 14.5

n.d. = not detected

[a] Reduced recoveries attributed to low solubility in RCM, volatility and/or metabolization of compounds; 100% recovery represents the complete retrieval of the amount of substance added. GC yields presented as mean values + SD [%] of biological replicates (n = 3). [b] GC yields represent the sum of geranic acid and nerolic acid; neral was not detected in biotransformations.

4.1.3. Production of (monoterpene) aldehydes by AlkJ and transformation *in vivo*

RCs of *E. coli* RARE (OD_{600} = 10.0) expressing (i) AlkJ or (ii) co-expressing AlkJ and LuxAB were produced as described above. The primary alcohols **4a** and **15a** were successfully oxidized, whereas (*R*)- and (*S*)-**16a** were moderately and poorly converted into the corresponding aldehydes, respectively (**b**; **Table S13**). Observed byproducts (indicated in red) included the corresponding CAs (**c**), formed by the further oxidation of aldehydes by (i) the metabolic background of *E. coli* or (ii) in combination with LuxAB. Other byproducts such as **15c** – formed from the substrate **16a** – indicate enoate reductase and aldehyde dehydrogenase activities.

Starting from **4a**, (*R*)-**16a** or (*S*)-**16a**, the amounts of the observed overoxidation products increased 1.3-fold (**4c**), 1.4-fold (**15c**) and 2.1-fold (**15c**), respectively; **15c** could be detected in traces in biotransformations starting from **15a** (**Table S13** and **Figure 6B** in the main article), which was not observed in reactions employing AlkJ alone (**Figure 6A**). Although subtle, these findings suggest a new enzymatic cascade transforming alcohols into carboxylates *via* two steps in living cells.

Table S12. Production of (monoterpene) aldehydes by AlkJ and transformation by LuxAB

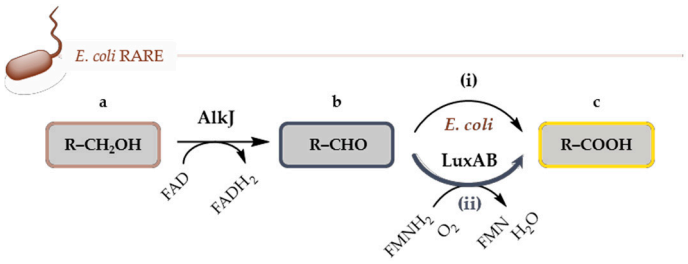

(i)

	Time	4a	4b	4c	2c	7c	Recovery [a]
Conversion of **4a**	0	83.7 ± 1.9	n.d.	n.d.	n.d.	n.d.	83.7 ± 1.9
	1	24.9 ± 1.4	8.6 ± 0.0	n.d.	n.d.	5.7 ± 1.1 [b]	39.2 ± 0.2
	24	n.d.	17.8 ± 2.4	17.6 ± 2.3	3.6 ± 0.4 [c]	8.0 ± 1.4 [b]	47.0 ± 3.4

	Time	15a	(*E*)-15b [d]	(*Z*)-15b [d]	15c		Recovery [a]
Oxidation of **15a**	0	52.2 ± 1.7	n.d.	n.d.	n.d.	-	52.2 ± 1.7
	1	70.2 ± 7.3	11.4 ± 1.5	6.6 ± 0.8	n.d.		88.2 ± 9.6
	24	9.9 ± 1.4	39.2 ± 4.8	44.5 ± 5.7	n.d.		93.6 ± 1.0

	Time	16a	16b	16c	15c		Recovery [a]
Oxidation of (*R*)-**16a**	0	98.5 ± 8.8	n.d.	n.d.	n.d.	-	98.5 ± 8.8
	1	95.1 ± 6.0	1.9 ± 0.1	n.d.	2.6 ± 0.5 [e]		97.0 ± 6.4
	24	55.5 ± 1.3	11.8 ± 10.3	n.d.	8.4 ± 1.6 [e]		73.0 ± 0.7

	Time	16a	16b	16c	15c		Recovery [a]
Oxidation of (*S*)-**16a**	0	47.1 ± 0.2	n.d.	n.d.	n.d.	-	47.1 ± 0.2
	1	70.5 ± 9.8	n.d.	n.d.	2.2 ± 1.0		72.6 ± 9.4
	24	86.8 ± 1.5	3.9 ± 0.3	n.d.	3.5 ± 0.3		94.2 ± 0.9

Table S12. Production of (monoterpene) aldehydes by AlkJ and transformation by LuxAB (continued)

(ii)

	Time	4a	4b	4c	2c	7c	Recovery [a]
Conversion of **4a**	0	97.8 ± 4.3	n.d.	n.d.	n.d.	n.d.	97.8 ± 4.3
	1	37.4 ± 2.8	10.4 ± 5.0	n.d.	n.d.	n.d.	47.8 ± 6.0
	24	15.5 ± 11.5	23.4 ± 15.5	23.5 ± 8.0	1.5 ± 1.1 [c]	n.d.	63.9 ± 10.4

	Time	15a	(*E*)-15b [d]	(*Z*)-15b [d]	15c		Recovery [a]
Oxidation of **15a**	0	56.6 ± 2.1	n.d.	n.d.	n.d.	-	56.6 ± 2.1
	1	68.1 ± 10.3	9.3 ± 1.6	5.2 ± 0.8	n.d.		86.4 ± 13.5
	24	22.8 ± 0.8	32.2 ± 0.5	34.9 ± 0.3	2.2 ± 0.1		89.9 ± 0.1

	Time	16a	16b	16c	15c		Recovery [a]
Oxidation of (*R*)-**16a**	0	96.3 ± 7.4	n.d.	n.d.	n.d.	-	96.3 ± 7.4
	1	99.6 ± 5.2	n.d.	n.d.	n.d.		99.6 ± 5.2
	24	73.0 ± 1.8	10.4 ± 0.9	n.d.	11.6 ± 0.6 [e]		95.0 ± 0.3

	Time	16a	16b	16c	15c		Recovery [a]
Oxidation of (*S*)-**16a**	0	64.0 ± 2.5	n.d.	n.d.	n.d.	-	64.0 ± 2.5
	1	87.0 ± 4.6	n.d.	n.d.	n.d.		87.0 ± 4.6
	24	86.5 ± 0.6	2.4 ± 0.2	n.d.	7.3 ± 0.2		96.1 ± 0.2

n.d. = not detected

[a] Reduced recoveries attributed to low solubility in RCM, volatility and/or metabolization of compounds; 100% recovery represents the complete retrieval of the amount of substance added. Byproduct forming enzymes are omitted for clarity in the scheme. GC yields presented as mean values + SD [%] of biological replicates (n = 3). [b] Metabolite of **4c** from fatty acid synthesis pathways [15]. [c] Metabolite of **4c** from fatty acid degradation through β-oxidation [16]. [d] The mixture of the *E*- and *Z*-isomers geranial and neral, respectively, is referred to as citral (see also: **Figure 6** in the main article). [e] GC yields represent the sum of geranic acid and nerolic acid.

4.2. Table of compounds

Table S13. List of compounds analyzed in this study

Compound	Retention time [min] [a] (CAS no.)			R =	Quantification method [b], [c]
	(a) R–CH_2OH	(b) R–CHO	(c) R–COOH		
1	n.a.	n.a.	2.431 (142-62-1)		n.a.
2	n.a.	n.a.	3.728 (124-07-2)		**4c**: 1.232 [b], [d]
3	n.a.	n.a.	4.437 (112-05-0)		n.a.
4	4.510–4.516 (112-30-1)	4.036 (112-31-2)	5.126–5.136 (334-48-5)		**4a**: 0.914, **b**: 1.495, **c**: 1.557 [b]
5	5.229 (112-42-5)	4.785 (112-44-7)	5.803 (112-37-8)		n.a.
6	5.943 (112-53-8)	5.492 (112-54-9)	6.442 (143-07-7)		**6c**: 1.232 [b], [e]
7	n.a.	n.a.	7.662 (544-63-8)		n.a.
8	2.870 (6920-22-5) [f]	n.a.	n.a.		n.a.
9	3.571 (629-11-8)	n.a.	n.a. (124-04-9)	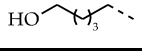	n.a.
10	4.297 (1117-86-8) [f]	n.a.	n.a.		n.a.
11	5.053 (629-41-4)	n.a.	n.a.	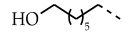	n.a.

Table S13. List of compounds analyzed in this study (continued)

12	n.a.	n.a.	n.a. (5129-58-8)		n.a.
13	n.a.	n.a.	8.619 (373-49-9) [g]	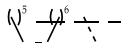	n.a.
14	n.a.	n.a.	6.429 (693-23-2)	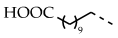	n.a.
15	4.385–4.401 (106-24-1) [h]	4.521 (5392-40-5) [i]	5.055 (459-80-3) [j]	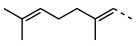	(*E*)-**15a**: 1.289, **b**: 0.964, **c**: 0.780 (*Z*)-**15a**: n.d., **b**: 0.595, **c**: 0.780 [b]
16	4.190–4.220 (1117-61-9) [k]	3.671 (2385-77-5) [l]	4.739 (18951-85-4) [m]	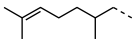	(*R*)-**16a**: 0.604, **b**: 1.015, **c**: 0.978 (*S*)-**16a**: 1.136, **b**: 1.105, **c**: 1.096 [b]
17	n.a.	n.a. (106-72-9) [n]	n.a.	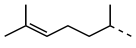	n.a.
18	n.a. (100-51-6)	n.a. (100-52-7)	n.a. (65-85-0)		n.a.
19	3.463 (60-12-8)	2.995 (122-78-1)	4.313 (103-82-2)		**19a**: k = 1.391, d = -0.051 / **b**: k = 0.912, d = 0.019 / **c**: k = 0.759, d = -0.098 [c]
20	4.660 (536-60-7)	4.340 (122-03-2)	5.500 (536-66-3)	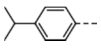	**20a**: k = 0.739, d = 0.014 / **b**: k = 0.774, d = 0.041 / **c**: k = 0.967, d = -0.059 [c]
21 [o]	4.766 (104-54-1)	4,546 (104-55-2)	5.518 (140-10-3)	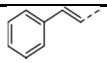	**21a**: 1.328, **b**: 1.329, **c**: 0.297 [b]
22	4.232 (122-97-4)	3.762 (104-53-0)	4.887 (501-52-0)	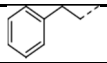	**22a**: 1.856 [b]
23	3.599–3.609 (89-95-2)	3.126–3.135 (529-20-4)	4.220–4.223 (118-90-1)		**23a**: 1.323, **b**: 1.370, **c**: 0.759 [b]
24	3.535 (587-03-1)	3.127 (620-23-5)	4.349 (99-04-7)		**24a**: k = 1.089, d = -0.041 / **b**: k = 1.157, d = 0.008 / **c**: k = 0.501, d = -0.069 [c]
25	3.535 (589-18-4)	3.219 (104-87-0)	4.413 (99-94-5)		**25a**: 1.312, **b**: 1.360, **c**: 0.876 [b]

n.a. = not available or not analyzed; CAS no. = Chemical Abstract Service registry number; n.d. = not detected

[a] Retention times for GC/FID; [b] calculation of GC yields based on RFFs as described above, methyl benzoate (CAS: 93-58-3) was used as IS (retention time: 3.340 min); [c] calculation of GC yields based on the measurement of compound solutions of different concentrations (0.1–4.0 mM) and linear regression (k = slope, d = intercept), $R^2 \geq 0.981$; [d] byproduct of fatty acid degradation (see also: **Table S12**); [e] byproduct related to fatty acid synthesis; [f] CAS no. referring to the racemic mixture; [g] palmitoleic acid = *cis*-9-hexadecenoic acid; [h] retention time and CAS refer to geraniol = (*E*)-3,7-dimethyl-2,6-octadien-1-ol; [i] retention time is given for geranial, the CAS no. refers to citral, a mixture of the *E*- and *Z*-isomers geranial and neral, respectively; neral could be attributed a retention time of 4.324 min; [j] retention time and CAS given for geranic acid = (*E*)-3,7-dimethylocta-2,6-dienoic acid; retention time of nerolic acid = (*Z*)-3,7-dimethyl-2,6-octadienoic acid: 4.834 min; [k] CAS referring to (*R*)-citronellol = (*R*)-3,7-dimethyl-6-octen-1-ol; CAS of (*S*)-citronellol = (*S*)-3,7-dimethyl-6-octen-1-ol: 7540-51-4; [l] CAS no. referring to (*R*)-citronellal = (*R*)-3,7-dimethyl-6-octenal; CAS of (*S*)-citronellal = (*S*)- 3,7-dimethyl-6-octenal: 5949-05-3; [m] CAS no. of (*R*)-citronellic acid = (*R*)-(+)-3,7-dimethyl-6-octenoic acid; CAS of (*S*)-citronellic acid = (*S*)-(−)-3,7-dimethyl-6-octenoic acid: 2111-53-7; [n] melonal = 2,6-dimethylhept-5-enal; [o] retention times and CAS no. refer to the *trans*-isomers of **21a–c**.

References

1. Li C, Wen A, Shen B, Lu J, Huang Y, Chang Y. FastCloning: A highly simplified, purification-free, sequence- and ligation-independent PCR cloning method. BMC Biotechnol. 2011;11:92-92. (DOI: https://doi.org/10.1186/1472-6750-11-92)
2. Wiesinger T, Bayer T, Milker S, Mihovilovic MD, Rudroff F. Cell factory design and optimization for the stereoselective synthesis of polyhydroxylated compounds. ChemBioChem. 2018;19(4):361-68. (DOI: https://doi.org/10.1002/cbic.201700464)
3. Zhang Y, Werling U, Edelmann W. SLiCE: A novel bacterial cell extract-based DNA cloning method. Nucleic Acids Research. 2012;40(8):e55-e55. (DOI:https://doi.org/10.1093/nar/gkr1288)
4. Santala S, Efimova E, Karp M, Santala V. Real-time monitoring of intracellular wax ester metabolism. Microbial Cell Factories. 2011;10(1):75. (DOI:https://doi.org/10.1186/1475-2859-10-75)
5. Lehtinen T, Efimova E, Santala S, Santala V. Improved fatty aldehyde and wax ester production by overexpression of fatty acyl-CoA reductases. Microbial Cell Factories. 2018;17(1):19. (DOI: https://doi.org/10.1186/s12934-018-0869-z)
6. Julsing MK, Schrewe M, Cornelissen S, Hermann I, Schmid A, Bühler B. Outer membrane protein AlkL boosts biocatalytic oxyfunctionalization of hydrophobic substrates in *Escherichia coli*. Applied and Environmental Microbiology. 2012;78(16):5724-33. (DOI:https://doi.org/10.1128/aem.00949-12)
7. Finnigan W, Thomas A, Cromar H, Gough B, Snajdrova R, Adams JP, Littlechild JA, Harmer NJ. Characterization of carboxylic acid reductases as enzymes in the toolbox for synthetic chemistry. ChemCatChem. 2017;9(6):1005-17. (DOI:https://doi.org/10.1002/cctc.201601249)
8. Akhtar MK, Turner NJ, Jones PR. Carboxylic acid reductase is a versatile enzyme for the conversion of fatty acids into fuels and chemical commodities. Proceedings of the National Academy of Sciences U. S. A. 2013;110(1):87-92. (DOI:https://doi.org/10.1073/pnas.1216516110)
9. Heath RS, Birmingham WR, Thompson MP, Taglieber A, Daviet L, Turner NJ. An engineered alcohol oxidase for the oxidation of primary alcohols. ChemBioChem. 2019;20(2):276-81. (DOI: https://doi.org/10.1002/cbic.201800556)
10. Kunjapur AM, Tarasova Y, Prather KLJ. Synthesis and accumulation of aromatic aldehydes in an engineered strain of *Escherichia coli*. Journal of the American Chemical Society. 2014;136(33):11644-54. (DOI: https://doi.org/10.1021/ja506664a)
11. del Solar G, Giraldo R, Ruiz-Echevarría MJ, Espinosa M, Díaz-Orejas R. Replication and control of circular bacterial plasmids. Microbiology and Molecular Biology Reviews. 1998;62(2):434-64. (DOI: https://doi.org/10.1128/mmbr.62.2.434-464.1998)
12. Studier FW. Protein production by auto-induction in high density shaking cultures. Protein expression and purification. 2005;41(1):207-34. (DOI:https://doi.org/10.1016/j.pep.2005.01.016)
13. Colepicolo P, Cho KW, Poinar GO, Hastings JW. Growth and luminescence of the bacterium *Xenorhabdus luminescens* from a human wound. Applied and Environmental Microbiology. 1989;55(10):2601-06. (DOI: https://doi.org/10.1128/AEM.55.10.2601-2606.1989)
14. Clark BC, Powell CC, Radford T. The acid catalyzed cyclization of citral. Tetrahedron. 1977;33(17):2187-91. (DOI: https://doi.org/10.1016/0040-4020(77)80002-1)
15. Janßen HJ, Steinbüchel A. Fatty acid synthesis in *Escherichia coli* and its applications towards the production of fatty acid based biofuels. Biotechnology for Biofuels. 2014;7(1):7. (DOI: https://doi.org/10.1186/1754-6834-7-7)
16. Jimenez-Diaz L, Caballero A, Segura A. Pathways for the degradation of fatty acids in bacteria. In: Rojo F, editor. Aerobic Utilization of Hydrocarbons, Oils and Lipids. Cham: Springer International Publishing; 2017. p. 1-23. (DOI: https://doi.org/10.1007/978-3-319-39782-5_42-1)